PROCEEDINGS OF SCIENCE

# The nonperturbative phase diagram of the bosonic BMN matrix model

**Samuel Kováčik***
*School of Theoretical Physics, Dublin Institute for Advanced Studies, 10 Burlington Road, Dublin 4, Ireland.*
*E-mail:* skovacik@stp.dias.ie

**Denjoe O'Connor**
*School of Theoretical Physics, Dublin Institute for Advanced Studies, 10 Burlington Road, Dublin 4, Ireland.*
*E-mail:* denjoe@stp.dias.ie

**Yuhma Asano**
*KEK Theory Center, High Energy Accelerator Research Organization, 1-1 Oho, Tsukuba, Ibaraki 305-0801, Japan.*
*E-mail:* yuhma@post.kek.jp

We study the thermal phase transition of the bosonic BMN model which is a mass deformed version of the bosonic part of the BFSS model. Our results connect the massless region of the phase diagram described by the bosonic BFSS model with the large-mass region, where the model is analytically solvable. We observe that at finite value of the matrix size N, the critical region is smeared over a small temperature range. The model has a single critical temperature, this arises as the large N limit of two apparent transitions at finite N. We emphasise the vital role played by finite N corrections in the confined phase and illustrate this with a novel treatment of the noninteracting Gaussian model.

*Corfu Summer Institute 2019 "School and Workshops on Elementary Particle Physics and Gravity" (CORFU2019)*
*31 August - 25 September 2019*
*Corfù, Greece*

*Speaker.





PoS(CORFU2019)221

## 1. Introduction

Dimensionally reduced Yang-Mills models are among the best candidates for testing the notorious gauge/gravity conjecture, the most researched example is the BFSS model [1, 2] and its maximally supersymmetric mass deformed version, the BMN model [3]. Bosonic and supersymetric models also arise from quantization of membranes and supermembranes on various backgrounds [1, 4].

This family of quantum matrix models, which can also be interpreted as models of interacting D0-branes, has a surprisingly rich phase structure including deconfining phase transitions as the temperature is varied [5, 6, 7, 8, 9, 10].

In the large-mass limit, the BMN model reduces to a gauged Gaussian model that can be solved analytically and has a single phase transition. At zero mass, based on the gauge/gravity duality conjecture, the model is connected to the Gregory-Laflamme [11, 12] transition. Our goal is to connect those two regimes nonperturbatively using numerical simulations.

The massless version of the model, the bosonic BFSS model, has been studied extensively both analytically and numerically [13, 14, 15, 16, 17, 18]. Initial studies reported two close thermal phase transitions which were in a good agreement with the results from $1/D$ ($D$ is the number of matrices) expansion performed in [14]. Later it was realised that in the large-$N$ limit there is only a single phase transition [18], which appears to be of the 1st order. Our study of the bosonic BMN model for $\mu = 2$ agrees with this conclusion [10].

In this paper we report our findings regarding the phase structure of the bosonic BMN model. At finite $N$, we observed two distinct phase transition which merge in the large-$N$ limit into a single one. Even though one of our approaches indicates that the transition is a standard 1st order one, showing clear signs of a transitioning two-level system, another approach suggests the transition might be more related to the Hagedorn transition. We leave this question open at this moment.

For $\mu = 2$ we gather enough data to extrapolate the results to the large-$N$ limit. For other values of $\mu$ we fixed $N = 12$ and produced a phase diagram with two (pseudo)critical temperatures for each value of $\mu$. These are expected to merge in the large-$N$ limit and their finite-$N$ values can serve as upper and lower boundaries for the large-$N$ critical temperature.

## 2. Model and observables

The gauged quantum model is defined using $D = 9$ Hermitian $N \times N$ matrices that transform as adjoint representation of $SU(N)$ and are placed on a thermal circle with the action defined as

$$S[X,A] = N \int_0^\beta d\tau \ \mathrm{Tr} \Bigg[ \ \tfrac{1}{2} D_\tau X^i D_\tau X^i - \tfrac{1}{4} \left( [X^r, X^s] + \tfrac{i\mu}{3} \varepsilon^{rst} X_t \right)^2 - \tfrac{1}{2} [X^r, X^m]^2 - \tfrac{1}{4} [X^m, X^n]^2 + \tfrac{1}{2} \left(\tfrac{\mu}{6}\right)^2 X_m^2 \Bigg], \tag{2.1}$$

where $i = 1, \dots, 9$; $r,s = 1,2,3$ and $m,n = 4, \dots, 8, 9$. The mass parameter is $\mu$, $\beta = 1/T$ is the inverse temperature and $D_\tau \cdot = \partial_\tau \cdot - i[A, \cdot]$ is the covariant derivative. The $SO(9)$ symmetry is explicitly broken to $SO(6)\times SO(3)$ by the mass terms and the cubic Myers term. We fixed $A$ to be diagonal and time independent which invokes the Vandermonde determinant described in [15].

Mean values of observables $\mathscr{O}$ are defined by path integration over Hermitian matrix elements as

$$\langle \mathscr{O}\rangle = \frac{\int [dX][dA]\ \mathscr{O}\ e^{-S[X,A]}}{Z},\ Z=\int [dX][dA]e^{-S[X,A]}. \tag{2.2}$$

We employ the usual lattice formulation where the matrices $X^i$ are placed on temporal nodes and $A$ on the links between them. The (Euclidean) time $\tau$ is discretised as $\tau \to \beta k/\Lambda$, where $k=1,\dots,\Lambda$. To reduce the discretisation effects from the kinetic term we use the method discussed in [9, 19]. The coupling constant has been fixed to 1 and all dimensional quantities are expressed in these natural units.

The standard set of observables for analysis of thermal phase transitions is the energy $E$, the specific heat $C_\mathrm{v}$, the extent of eigenvalues $\langle R^2\rangle$ and the Polyakov loop $\langle |P|\rangle$ which serves as an order parameter in the deconfining transition. The Myers observable, $M$, is important in the supersymmetric formulation of the model as fermionic degrees of freedom can stabilise fuzzy-sphere configurations [9], we have not not observed such behaviour in the bosonic model. The list of observables follows:

$$\begin{aligned}
E &= N^{-2}(-\partial_\beta)\log Z,\\
C_\mathrm{v} &= \beta^2\partial_\beta^2\log Z,\\
\langle |P|\rangle &= \left\langle \frac{1}{N}\left|\mathrm{Tr}\ (\exp(i\beta A))\right|\right\rangle,\\
\langle R^2\rangle &= \left\langle \frac{1}{N\beta}\int_0^\beta d\tau\ \mathrm{Tr}\ \left(X^iX^i\right)\right\rangle,\\
M &= \left\langle \frac{i}{3N\beta}\int_0^\beta d\tau\ \varepsilon^{rst}\ \mathrm{Tr}\ \left(X^rX^sX^t\right)\right\rangle.
\end{aligned} \tag{2.3}$$

Typical behaviour of these observables is shown in the figures 1 and 2. We have also introduced two new observables that improve the accuracy of measurements of (pseudo)critical temperatures for finite values of $N$. We performed Hybrid Monte Carlo (HMC) simulations of the system to evaluate the path integrals and noticed that close to the apparent transition temperature, the system transitions between two distinct levels, one close to $\langle |P|\rangle \approx 1/N$ and one close to $\langle |P|\rangle \approx 1/2$. At low temperature, the system spends the entire Monte Carlo time at the bottom level, but as the temperature is increased it tends to spend larger portion of it in the top one. Therefore, we defined the observable $\mathbb{P}$ that captures which level is preferred by the system at a given temperature defined by

$$\mathbb{P}_x = \int_x^1 \mathscr{P}(q)dq,\quad \text{with}\quad \mathbb{P}_{0.5}=\mathbb{P}, \tag{2.4}$$

where $\mathscr{P}(q)$ is the probability distribution for the Polyakov loop. Quite surprisingly, this observable shows a very clear piecewise linear behaviour, see the figure 3 [1]. It is constant well bellow and

[1] We have tested that using $\mathbb{P}_{0.4}$ or $\mathbb{P}_{0.3}$ yields similar results.

above the transition and linear in the middle of it. We take the root of the linear function describing the transition region to be $T_{c1}$. As the steepness of this line increases with $N$ indefinitely, values of $T_{c1}$ defined by any point on it converge to the same value. The second introduced observable is

$$\langle |P_n| \rangle = \left\langle \frac{1}{N} \left| \text{Tr } (\exp(in\beta A)) \right| \right\rangle. \tag{2.5}$$

This observable for $n > 2$ captures the behaviour of higher moments of the eigenvalue distribution of $A$ expressed as $u_n = \int_{-\pi}^{\pi} \rho(\theta) e^{in\theta} d\theta$. In the zero-temperature limit, the eigenvalues of $A$ are distributed uniformly, $u_n = 0$ for $n \geq 1$. Then, with increasing temperature, the distribution becomes nonuniform, $u_1 > 0$ while $u_2 = u_3 = ... = 0$. With further increasing temperature, the distribution develops a gap, all moments become excited or equivalently $\langle |P_n| \rangle > 0$ for $n \geq 1$. For all values of $N$ we observe a very sharp change in the behaviour of $\langle |P_2| \rangle$. It is constant below a certain temperature and then start growing above it. We denote this temperature $T_{c2}$. Higher modes $\langle |P_n| \rangle$, $n = 3, 4, ...$ are growing as well, but at a slower rate than $\langle |P_2| \rangle$ so we use it to mark the transition.

## 3. Thermal phase transition(s)

The figure 1 shows the behaviour of the observables for $\mu = 2$, $N = 32$ and $\Lambda = 24$. We can clearly see that the system undergoes either one or more (closely separated) phase transitions around $T \sim 0.92$. Measurements of the Polyakov loop and specific heat for increasing values of $N$ are shown in figure 2, confirming that the transition region shrinks in the large-$N$ limit and the scaling of $C_V^{\max}$ signals a 1st order phase transition.

Let us now focus on the case of $\mu = 2$, $N = 32$ and $\Lambda = 24$. The root of the growing linear function in the left panel of figure 3 is taken to be at the first (pseudo)critical temperature, $T_{c1}$, where the underlying eigenvalue distribution becomes nonuniform. The bending point in the function in the right panel, which is measured as a crossing point of two linear fits, is taken to be at the second (pseudo)critical temperature, $T_{c2}$, where the eigenvalue distribution becomes gapped. Details of this behaviour are discussed in [10].

We have measured the values of $T_{c1}$ and $T_{c2}$ for $N = 12, 24, 32, 48$ and extrapolated them to infinite $N$, the results are shown in the figure 4. The (pseudo)critical temperatures merge into a single one, the exact value depends only slightly on the choice of the fitting function. The best agreement is for the quadratic fit, yielding $T_{c1} \to 0.9137(9)$ and $T_{c2} \to 0.914(2)$ in the large-$N$ limit.

The critical temperature can be approximately obtained even with a single, possibly small, value of $N$. To do so, one needs to have a good theoretical prediction for $\langle |P| \rangle$ as a function of $T$ with finite-$N$ corrections included. We used

$$\langle |P| \rangle (T) = P_0 + \sqrt{\frac{\langle l \rangle_N}{N}} e^{-m\left(T^{-1} - T_H^{-1}\right)} \text{ for } T < T_H \tag{3.1}$$

$$\langle |P| \rangle (T) = \frac{1}{2} \frac{e^{m\left(T^{-1} - T_H^{-1}\right)}}{1 - \sqrt{1 - m\left(T^{-1} - T_H^{-1}\right)}} \text{ for } T > T_H. \tag{3.2}$$

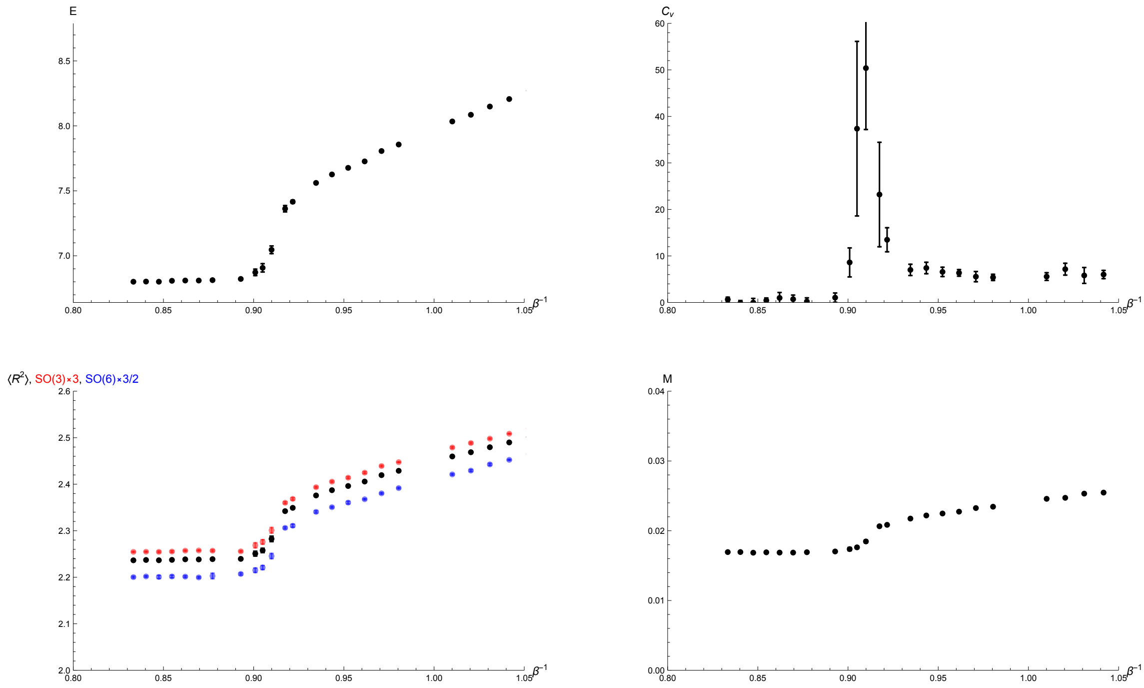


**Figure 1:** Observables of the model for $\mu = 2$, $N = 32$ and $\Lambda = 24$. The Myers observable seems to be negligible and copies the shape of $\langle R^2\rangle$. All observables point to either a single or multiple transitions around $T \approx 0.92$. The split between $SO(3)$ and $SO(6)$ components of $\langle R^2\rangle$ is due to different masses.

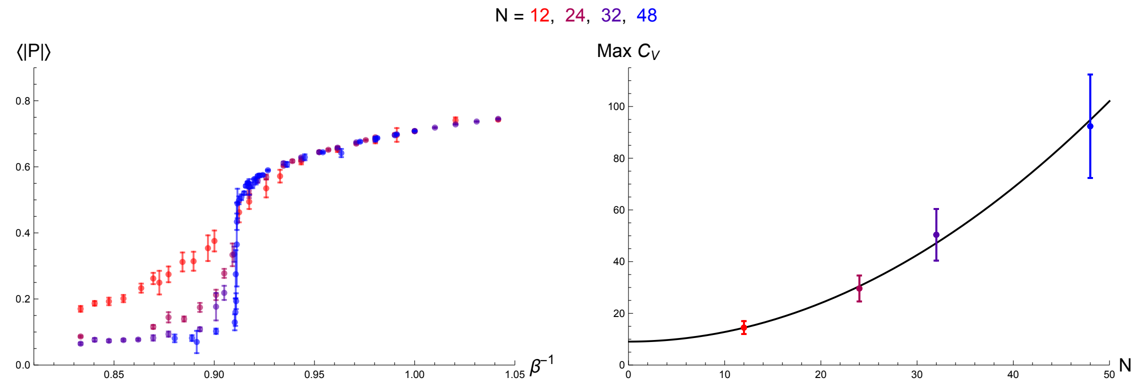


**Figure 2:** The evolution of the Polyakov loop $\langle|P|\rangle$ for $\mu = 2$, $\Lambda = 24$ with increasing $N$. The transition region becomes sharper with larger $N$. The right figure grows as $C_V^{\max} = 9.1(8) + 0.037(2)N^2$.

Here, $\langle l\rangle_N = \frac{e^{m\left(T_H^{-1}-T^{-1}\right)}}{1-e^{m\left(T_H^{-1}-T^{-1}\right)}} - \frac{c\ e^{\left(T_H^{-1}-T^{-1}\right)c\ m\ N^2} N^2}{1-e^{\left(T_H^{-1}-T^{-1}\right)c\ m\ N^2}}$, $m = T_H \ln 9$ and $c$ is chosen so the two functions meet at $T = T_H$. This is obtained in the Hamiltonian approach to the gauge Gaussian model, [6, 20] and will be discussed in our forthcoming work [21]. $T_H$ is to be interpreted as the Hagedorn temperature and we have measured its values for $N = 12,\ 24,\ 32,\ 48$ as $T_H = 0.924(1),\ 0.9167(4),\ 0.9136(3),\ 0.9127(2)$. This is very close to the results obtained from the previous method of extrapolating two (pseudo)critical temperatures. The values of $P_0$ are zero-

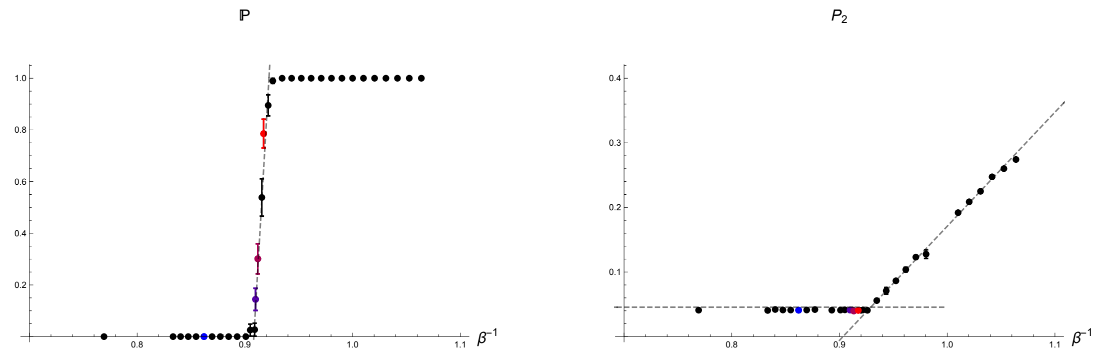


**Figure 3:** Values of $\mathbb{P}$ and $\langle|P_2|\rangle$ for $\mu = 2$, $N = 32$ and $\Lambda = 24$ and increasing value of temperature $T = \beta^{-1}$. The points in the transition region in the left plot were fit by a linear function whose slope increases with $N$. The four coloured points correspond to $T = 0.8621,\ 0.9099,\ 0.9120$ and $0.9174$.

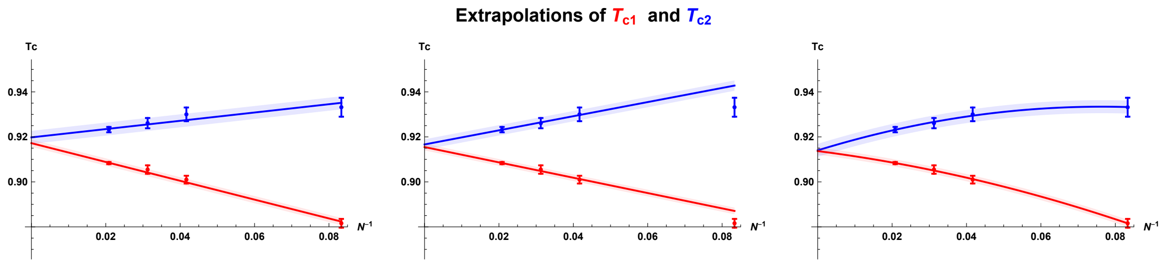


**Figure 4:** Extrapolations of the (pseudo)critical temperatures from results obtained from $N = 12,\ 24,\ 32,\ 48$. The left plot is using a linear fit, the middle plot is using linear fit while omitting $N = 12$ value, the right one is using a quadratic fit. All fits are performed functions of $N^{-1}$.

temperature contributions to $\langle|P|\rangle$ and are understood to be only finite-$N$ effects, their values for $N = 12,\ 24,\ 32$ are $P_0 = 0.058(4),\ 0.028(2),\ 0.008(3)$. We have set $P_0 = 0$ for $N = 48$ as we did not obtain enough data points for $T \ll T_H$.

The same two methods can be applied to the model for any value of $\mu$. At $\mu = 0$ the model is just the bosonic part of the BFSS model which has been well researched both theoretically and numerically. At first, it was believed that there are two, closely separated phase transitions, one of the 2nd and one of the 3rd order. The latest research [18], however, reports only a single 1st order phase transition. Our $\mu = 2$ extrapolations to infinite $N$ are in an agreement with a single phase transition which seems to be of the nature of the Hagedorn phase transition, see the figure 5.

We have performed a detailed study of the gauge Gaussian model with $\mu = 2$ and shown that the leading finite-$N$ effects in the low temperature phase are substantial. The results are shown in the figure 6. The solid curves are those described by $\langle l\rangle_N$ discussed above where $\langle l\rangle_N$ uses the sharp cutoff on states in the Hamiltonian formulation described by words of length $cN^2 - 1$ and $\langle l\rangle_N$ describes the mean word length, see [6, 20].

For large values of $\mu$, only the quadratic terms contribute and the model effectively reduces to a gauged Gaussian model that has a single critical temperature located at $T_c = \frac{\mu}{6\ln\left(3+2\sqrt{3}\right)}$.

We have produced the phase diagram for $N = \Lambda = 24$, it is shown in the figure 7. The gray points mark two (pseudo)critical temperatures measured using $\langle|P_2|\rangle$ and $\mathbb{P}$, the red poins show the

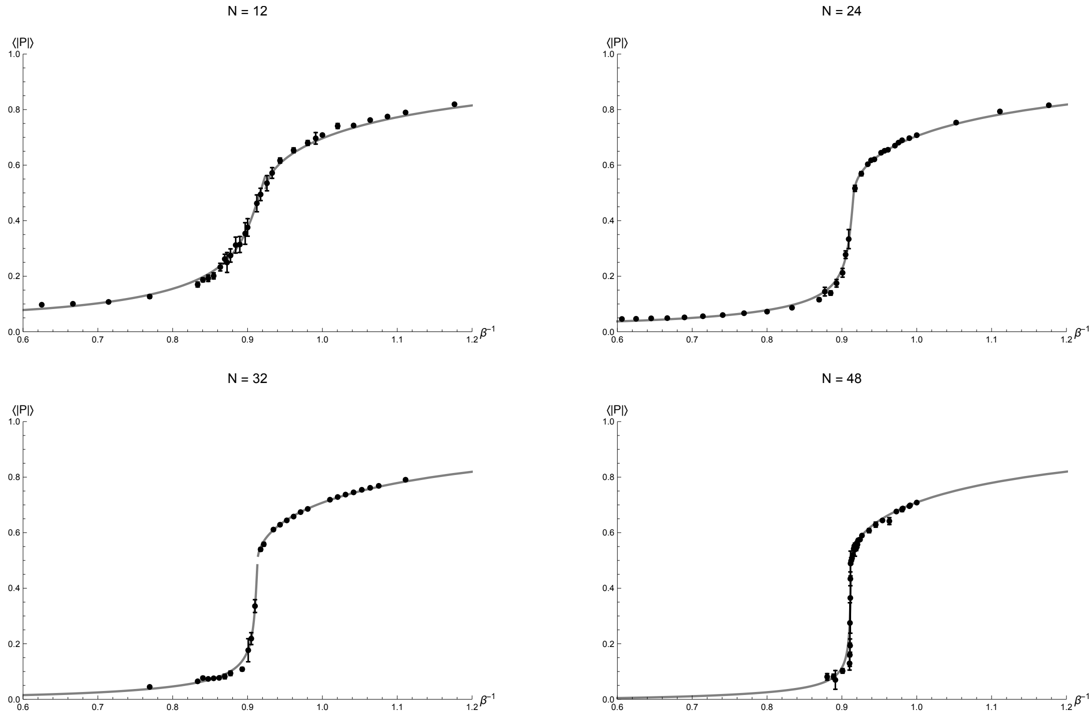


**Figure 5:** Numerically obtained values of $\langle|P|\rangle$ for $\mu = 2, \Lambda = 24$ and various values of $N$. The solid lines are fits using theoretical predictions 3.1 and 3.2 with parameters $T_H$ and $P_0$ obtained by fitting.

critical temperature measured by $T_H$, which, as expected, lay between the other two. The dashed line shows the large-$\mu$ critical temperature which the points asymptote to.

## 4. Conclusions

We have analysed the behaviour of the bosonic BMN matrix model, focusing on the thermal deconfining phase transition at finite $\mu$. We observed that at finite $N$ we can distinguish two closely separated (pseudo)critical temperatures $T_{c1}$ and $T_{c2}$. At $T > T_{c1}$ the system prefers states with $\langle|P|\rangle \geq 1/2$ and the eigenvalue distribution is nonuniform. At $T > T_{c2}$ higher moments of the eigenvalue distribution develops nontrivial expectation values, the distribution is gapped. We have also observed that these two (pseudo)critical temperatures merge into one in the large-$N$ limit.

We were able to fit the data for Polyakov loop $\langle|P|\rangle$ using functions obtained from a theoretical description of the model at finite $N$. The fitting parameter $T_H$ is to be interpreted as the Hagedorn temperature (details will be discussed in our upcoming work), which is consistent with the aforementioned single large-$N$ critical temperature.

Exact nature of the phase transition remains unclear at this point. Analysing the Monte Carlo trajectories of the system shows clear signs of two-level system well approximated by two Gaussian distributions [22, 23]. However, fitting using 3.1 and 3.2 shows a clear relation to the Hagedorn phase transition as well.

For a single finite value of $N$, we have constructed the phase diagram, which interpolates smoothly between the zero-mass BFSS prediction and large-mass prediction of the gauged Gaus-

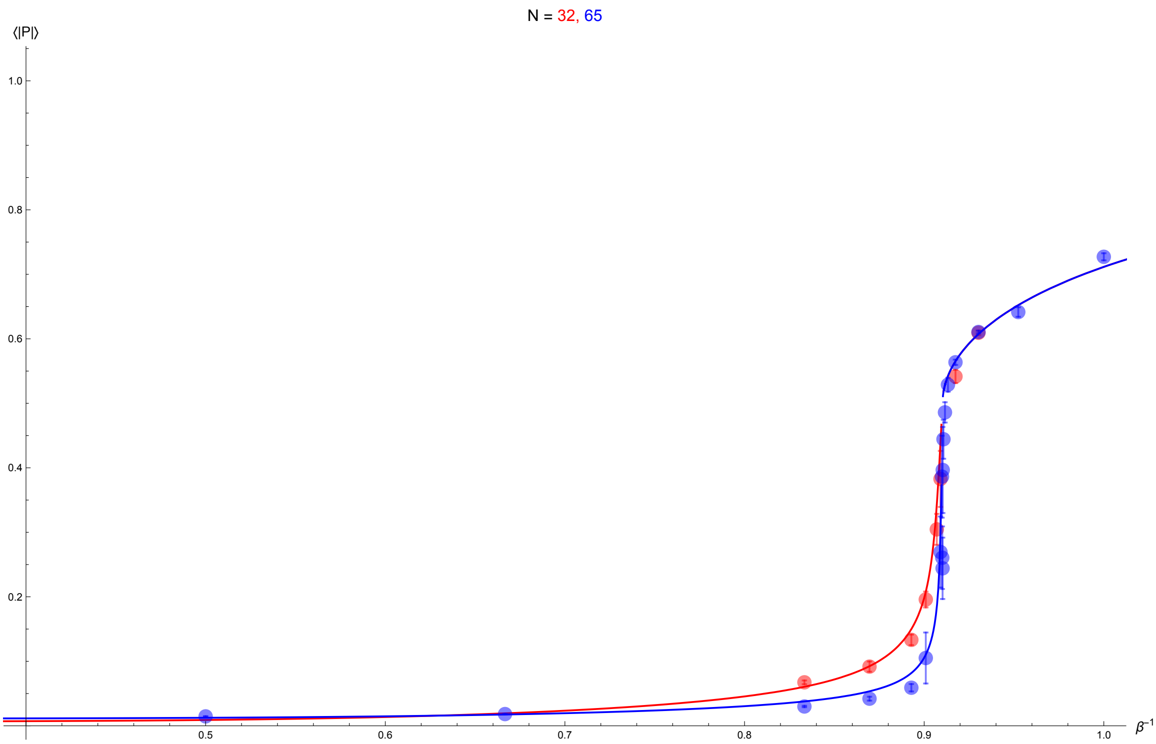


**Figure 6:** We have tested the theoretical predictions 3.1 and 3.2 also for the pure Gaussian model with $\mu = 2$ for which the critical temperature is known exactly. In these plots we have set $P_0 = 0$.

sian model. It is plausible that in the large-$N$ limit the two (pseudo)critical temperatures shown in 7 merge into one, possible close to the value predicted by the Hagedorn fit (red points in the same diagram). In [10] we have also tested that with our lattice formulation the results depend only very weakly on lattice parameter $\Lambda$ and are reasonably close to the continuum value.

Our choice of the fitting function, equations 3.1 and 3.2, contained a contribution from the $T \to 0$ behaviour of the Polyakov loop, denoted $P_0$. We know that in this limit the eigeinvalues of $A$ are uniformly distribution over the entire interval. We can model them as a set of random numbers $\theta_i = \frac{2\pi i}{N} + f$ where $i = 1, \ldots, N$ and $f$ is a random number that describes their fluctuations. We can take $f$ to be random with central Gaussian distribution with $\sigma = \frac{2\pi a}{N}$. This way, $N$ and $a$ determine the value of $\langle |P| \rangle$.

For $N = 12,\ 24,\ 32$ we have obtained, for the data at the lowest measured temperatures ($\beta = 2.2,\ 1.85,\ 1.7$) the values of $a$ and used it to compute $P_0$. The results of the calculation ($0.082,\ 0.043,\ 0.029$) are very close to the values of $\langle |P| \rangle$ measured at those temperatures ($0.08(2),\ 0.0427(9),\ 0.034(1)$). Given the knowledge of $a$, we can estimate the value of $P_0$ rather precisely.

The next step is, instead of measuring $a$, to have a theoretical estimate for it. The dominant effect in the zero-temperature limit is the logarithmic repulsion between the eigenvalues. If an eigenvalue is positioned between two others, separated by a distance of $a\frac{2\pi}{N}$ from each of them, it will be moving in an effective potential $U(x) = U_0 - \frac{x^2}{\left(a\frac{2\pi}{N}\right)^2} + \ldots$. This means that the dispersion is proportional to the separation and we should take $a = 2^{-1/2}$. Actually, as the logarithmic force

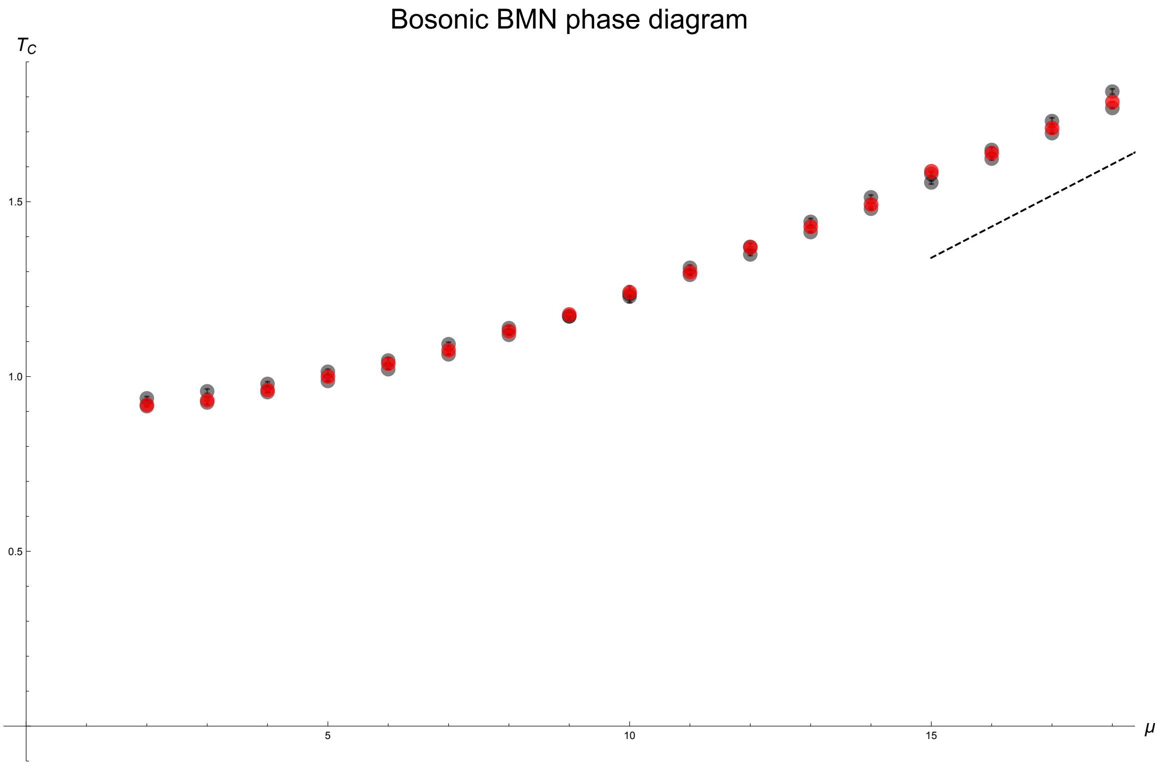


**Figure 7:** The (pseudo)critical temperatures for $N = \Lambda = 24$. The gray points were obtained using $\mathbb{P}$ and $\langle|P_2|\rangle$. The red points were obtained by measuring $T_H$ using 3.1 and 3.2. The dashed line shows the large-$\mu$ prediction $T_c = \frac{\mu}{6\ln\left(3+2\sqrt{3}\right)}$.

decays rather slowly, we should take other eigenvalues into account as well, changing the estimate to $a = 2^{-1/2}(1+1/2+1/4+\ldots+1/(N/2)^2 = 2^{-1/2}H(N/2,2)$, where $H$ is a harmonic number. This yields, given only $N$, the estimate for $\langle|P|\rangle$ as $0.13, 0.052, 0.035$ which, given the the bold estimates, is reasonably close to the measured values. Therefore, we believe that describing the low temperature behaviour of $A$ using a set of uniformly separated eigenvalues fluctuating around their mean positions in the presence of logarithmic repulsion is accurate.

Our results are in a broad agreement with $1/D$ studies [17, 25] but does not match it exactly as the authors observe two closely separated phase transitions. As a recent numerical study of the BFSS model [18] also reports a single phase transition, we believe that by including higher terms in the $1/D$ expansion, the two phase transitions would merge into a single one in this approximation as well.

A possible line of future research is the study of bosonic version of the D0–D4 Berkooz-Douglas model [26, 27, 28]. The model has degrees of freedom that transform under the fundamental representation of $SU(N_f)$ and the work [9] reported exceptional behaviour for $N_f = 2N$ which should be interesting to study in the bosonic model.

## Acknowledgment

The authors wish to thank the Corfu Summer Institute for its hospitality and acknowledge the

Irish Centre for High-End Computing (ICHEC) for the provision of computational facilities and support (Projects dsphy009c, dsphy010c and dsphy012c). The support from Action MP1405 QSPACE of the COST foundation is gratefully acknowledged. Y. Asano is supported by the JSPS Research Fellowship for Young Scientists. S. Kováčik was supported by Irish Research Council funding. The authors would like to thank G. Bergner, M. Hanada, G. Ishiki, T. Morita and H. Watanabe for valuable discussion.

## References

[1] B. de Wit, J. Hoppe and H. Nicolai, "On the Quantum Mechanics of Supermembranes," Nucl. Phys. B **305** (1988) 545. doi:10.1016/0550-3213(88)90116-2

[2] T. Banks, W. Fischler, S. H. Shenker and L. Susskind, "M theory as a matrix model: A Conjecture," Phys. Rev. D **55**, 5112 (1997) [hep-th/9610043].

[3] D. E. Berenstein, J. M. Maldacena and H. S. Nastase, "Strings in flat space and pp waves from N=4 super Yang-Mills," JHEP **0204** (2002) 013 doi:10.1088/1126-6708/2002/04/013 [hep-th/0202021].

[4] N. Kim and J. H. Park, "Massive super Yang-Mills quantum mechanics: Classification and the relation to supermembrane," Nucl. Phys. B **759** (2006) 249 doi:10.1016/j.nuclphysb.2006.10.005 [hep-th/0607005].

[5] O. Aharony, J. Marsano, S. Minwalla, K. Papadodimas and M. Van Raamsdonk, "The Hagedorn - deconfinement phase transition in weakly coupled large N gauge theories," Adv. Theor. Math. Phys. **8** (2004) 603 doi:10.4310/ATMP.2004.v8.n4.a1 [hep-th/0310285].

[6] K. Furuuchi, E. Schreiber and G. W. Semenoff, "Five-brane thermodynamics from the matrix model," hep-th/0310286.

[7] G. W. Semenoff, "Black holes and thermodynamic states of matrix models," In *Shifman, M. (ed.) et al.: From fields to strings, vol. 3* 2009-2034

[8] O. Aharony, J. Marsano, S. Minwalla, K. Papadodimas, M. Van Raamsdonk and T. Wiseman, "The Phase structure of low dimensional large N gauge theories on Tori," JHEP **0601** (2006) 140 doi:10.1088/1126-6708/2006/01/140 [hep-th/0508077].

[9] Y. Asano, V. G. Filev, S. Kováčik and D. O'Connor, "The non-perturbative phase diagram of the BMN matrix model," JHEP **1807** (2018) 152 doi:10.1007/JHEP07(2018)152 [arXiv:1805.05314 [hep-th]].

[10] Y. Asano, V. G. Filev, S. Kováčik and D. O'Connor, "The Confining Transition in the Bosonic BMN Matrix Model," preprint [arXiv:2001.03749 [hep-th]].

[11] R. Gregory and R. Laflamme, "Black strings and p-branes are unstable," Phys. Rev. Lett. **70** (1993) 2837 doi:10.1103/PhysRevLett.70.2837 [hep-th/9301052].

[12] R. Gregory and R. Laflamme, "The Instability of charged black strings and p-branes," Nucl. Phys. B **428** (1994) 399 doi:10.1016/0550-3213(94)90206-2 [hep-th/9404071].

[13] O. Aharony, J. Marsano, S. Minwalla and T. Wiseman, "Black hole-black string phase transitions in thermal 1+1 dimensional supersymmetric Yang-Mills theory on a circle," Class. Quant. Grav. **21** (2004) 5169 doi:10.1088/0264-9381/21/22/010 [hep-th/0406210].

[14] N. Kawahara, J. Nishimura and S. Takeuchi, "Phase structure of matrix quantum mechanics at finite temperature," JHEP **0710** (2007) 097 doi:10.1088/1126-6708/2007/10/097 [arXiv:0706.3517 [hep-th]].

[15] V. G. Filev and D. O'Connor, "The BFSS model on the lattice," JHEP **1605** (2016) 167 doi:10.1007/JHEP05(2016)167 [arXiv:1506.01366 [hep-th]].

[16] T. Azuma, T. Morita and S. Takeuchi, "Hagedorn Instability in Dimensionally Reduced Large-N Gauge Theories as Gregory-Laflamme and Rayleigh-Plateau Instabilities," Phys. Rev. Lett. **113** (2014) 091603 doi:10.1103/PhysRevLett.113.091603 [arXiv:1403.7764 [hep-th]].

[17] G. Mandal, M. Mahato and T. Morita, "Phases of one dimensional large N gauge theory in a 1/D expansion," JHEP **1002** (2010) 034 doi:10.1007/JHEP02(2010)034 [arXiv:0910.4526 [hep-th]].

[18] G. Bergner, N. Bodendorfer, M. Hanada, E. Rinaldi, A. Schäfer and P. Vranas, "Thermal phase transition in Yang-Mills matrix model," [arXiv:1909.04592 [hep-th]].

[19] Y. Asano and D. O'Connor *In preparation.*

[20] S. Hadizadeh, B. Ramadanovic, G. W. Semenoff and D. Young, "Free energy and phase transition of the matrix model on a plane-wave," Phys. Rev. D **71** (2005) 065016 doi:10.1103/PhysRevD.71.065016 [hep-th/0409318].

[21] Y. Asano, S. Kováčik and D. O'Connor *In preparation.*

[22] M. E. Fisher and A. N. Berker, "Scaling for first-order transitions in thermodynamic and finite systems," Phys. Rev. B **26**, 2507 (1982). doi:10.1103/PhysRevB.26.2507

[23] D. P. Landau and K. Binder, "Finite-size scaling at first-order phase transitions" Phys. Rev. B **30** (1984) 1477. doi:10.1103/PhysRevB.30.1477

[24] M. S. S. Challa, D. P. Landau and K. Binder, "Finite size effects at temperature driven first order transitions," Phys. Rev. B **34** (1986) 1841. doi:10.1103/PhysRevB.34.1841

[25] S. Takeuchi, "D-dependence of the gap between the critical temperatures in the one-dimensional gauge theories," Eur. Phys. J. C **79** (2019) no.7, 548 doi:10.1140/epjc/s10052-019-6941-y [arXiv:1712.09261 [hep-th]].

[26] V. G. Filev and D. O'Connor, "A Computer Test of Holographic Flavour Dynamics," JHEP **1605** (2016) 122 doi:10.1007/JHEP05(2016)122 [arXiv:1512.02536 [hep-th]].

[27] Y. Asano, V. G. Filev, S. Kováčik and D. O'Connor, "The Flavoured BFSS Model at High Temperature," JHEP **1701** (2017) 113 doi:10.1007/JHEP01(2017)113 [arXiv:1605.05597 [hep-th]].

[28] Y. Asano, V. G. Filev, S. Kováčik and D. O'Connor, "A computer test of holographic favour dynamics. Part II," JHEP **1803** (2018) 055 doi:10.1007/JHEP03(2018)055 [arXiv:1612.09281 [hep-th]].

PoS(CORFU2019)221